

# SDSS-IV MaNGA: Non-Regular Rotators Quench Faster than Regular Rotators

R. J. Smethurst,<sup>1</sup> M. Merrifield,<sup>1</sup> K. L. Masters,<sup>2</sup> C. J. Lintott,<sup>3</sup>  
A.-M. Weijmans,<sup>4</sup> et al.

<sup>1</sup> *School of Physics and Astronomy, The University of Nottingham, University Park, Nottingham, NG7 2RD, UK*

<sup>2</sup> *Institute of Cosmology and Gravitation, University of Portsmouth, Dennis Sciama Building, Barnaby Road, Portsmouth, PO1 3FX, UK*

<sup>3</sup> *Oxford Astrophysics, Department of Physics, University of Oxford, Denys Wilkinson Building, Keble Road, Oxford, OX1 3RH, UK*

<sup>4</sup> *School of Physics and Astronomy, University of St Andrews, North Haugh, St Andrews, Fife, KY16 9RJ, UK*

25 May 2017

## ABSTRACT

With data from the MaNGA IFU survey, we construct a sample of regular rotators which have been matched in stellar mass to a sample of non-regular rotators, resulting in 314 galaxies total, which all lie off the star forming sequence. We use  $u - r$  and  $NUV - u$  colours from SDSS and GALEX and an existing inference package, STARPY to conduct a ‘first look’ at the time and exponentially declining rate that quenching occurs in these galaxies. We find that quenching is more likely to occur at a rapid rate for non-regular rotators than across the regular rotator sample. The distribution of quenching rates across the two populations is significantly ( $3.6\sigma$ ) different, suggesting that regular and non-regular rotators do indeed have different evolutionary histories. We discuss how the total gas mass of a merger, rather than the merger mass ratio, may decide a galaxy’s ultimate kinematic fate.

**Key words:** galaxies – photometry, galaxies – statistics, galaxies – morphology

## 1 INTRODUCTION

Recent work studying the early-type galaxy population has revealed that it is actually composed of two separate populations. The majority of early-types are rotationally supported (Emsellem et al. 2011) with  $\sim 7$  times the number of regular (or ‘fast’) rotators, with kinematic discs, than non-regular (or ‘slow’) rotators, with dispersion dominated kinematics (Cappellari et al. 2007; Emsellem et al. 2007). This has led to the proposal of a revision of Hubble’s morphological classification scheme in the form of a ‘comb’ (Cappellari 2016), whereby the evolution of a galaxy, from disc to bulge-dominated, takes place along a ‘tine’ of the comb as a regular rotator, always retaining an underlying disc. If the discs of these regular rotators are somehow destroyed, they then evolve along the ‘handle’ of the comb to become non-regular rotators.

Dry major mergers are considered the most likely process to produce non-regular rotators (Duc et al. 2011; Naab et al. 2014) as they can rapidly destroy the disc dominated nature of a galaxy (Toomre & Toomre 1972). Regular rotators, are thought to evolve from the slow build up of a galaxy’s bulge over time, eventually overwhelming the disc. This growth is thought to occur via gas-rich major or minor mergers (Duc et al. 2011) and by gas accretion (Cappellari et al. 2013; Johnston et al. 2014) which can produce a bulge

dominated but rotationally supported galaxy (which would traditionally have been visually classified as an early-type in the Hubble classification scheme).

Both major mergers and minor mergers have been postulated as quenching mechanisms (Hopkins et al. 2008b; Snyder et al. 2011; Hayward et al. 2014), with major mergers thought to cause a much faster quench of the remnant galaxy than a minor merger (Lotz et al. 2008, 2011). Gas accretion is also thought to cause quenching, as the large gravitational potential of the bulge that builds as the accreted gas sinks to the centre of the galaxy prevents the disc from collapsing and forming stars (Fang et al. 2013). If regular and non-regular rotators are formed evolve via these different mechanisms, we should therefore also expect to find a difference in the star formation histories of quenched regular and non-regular rotators.

In this letter, we conduct a first look at this problem using an existing Bayesian star formation inference package, STARPY, to determine the quenching histories of a sample of regular and non-regular rotators. We use broadband optical,  $u - r$  and near-ultraviolet  $NUV - u$  colours from SDSS and GALEX to infer both the time and rate that quenching has occurred in each galaxy. We aim to determine whether regular and non-regular rotating galaxies have different quenching histories. The zero points of all magnitudes are in the AB system. Where necessary, we adopt the

WMAP Seven-Year Cosmology (Jarosik et al. 2011) with  $(\Omega_m, \Omega_\Lambda, h) = (0.26, 0.73, 0.71)$ .

## 2 DATA AND METHODS

### 2.1 SDSS & GALEX Photometry

We obtain optical photometry from the Sloan Digital Sky Survey Data Release 7 (SDSS; York et al. 2000; Abazajian et al. 2009). We utilise the Petrosian magnitude, `petroMag`, values for the  $u$  (3543Å) and  $r$  (6231Å) wavebands provided by the SDSS DR7 pipeline (Stoughton et al. 2002). Further to this, we also required NUV (2267Å) photometry from the GALEX survey (Martin et al. 2005). Observed fluxes are corrected for galactic extinction (Oh et al. 2011) by applying the Cardelli, Clayton, & Mathis (1989) law. We also adopt  $k$ -corrections to  $z = 0.0$  and obtain absolute magnitudes from the NYU-VAGC (Blanton et al. 2005; Padmanabhan et al. 2008; Blanton & Roweis 2007).

### 2.2 MaNGA Survey & Data Reduction Pipeline

MaNGA is a multi-object IFU survey conducted with the 2.5 m Sloan Foundation Telescope (Gunn et al. 2006) at Apache Point Observatory (APO). By 2020 MaNGA will have acquired IFU spectroscopy for  $\sim 10000$  galaxies, all with  $M_* > 10^9 M_\odot$  and an approximately flat mass selection (Wake et al., in preparation). The target selection does not include any cuts on morphology, colour or environment.

In order to obtain spectra, MaNGA makes use of the Baryon Oscillation Spectroscopic Survey (BOSS) spectrograph (Smeed et al. 2013). The BOSS spectrograph provides continuous coverage between 3600 Å and 10300 Å at a spectral resolution  $R \sim 2000$  ( $\sigma_{\text{instrument}} \sim 77 \text{ km s}^{-1}$ ).

Complete spectral coverage to  $1.5R_e$ , a galaxy's effective radius, is obtained for the majority of targets, though a subset have coverage to  $2.5R_e$ . See Bundy et al. (2015) for an overview of the MaNGA survey. For a further description of the instrumentation used by MaNGA see Drory et al. (2015). For a detailed description of the observing strategy see Law et al. (2015) and for description of the survey design see Yan et al. (2016).

The raw data was processed by the MaNGA data reduction pipeline (DRP), which is discussed in detail Law et al. (2016). The MaNGA DRP extracts, wavelength calibrates and flux calibrates all fibre spectra obtained in every exposure. The individual fibre spectra are then used to form a regular gridded datacube of  $0.5''$  spaxels and spectral channels. The spectra are logarithmically sampled with bin widths of  $\log \lambda = 10^{-4}$ .

These datacubes are then analysed using the MaNGA data analysis pipeline (DAP); the development of which is ongoing and will be described in detail in Westfall et al. (in preparation). The primary output from the DAP are 2D “maps” (i.e., images) of measured properties, which include flux, stellar-continuum fits, absorption- and emission-line properties, spectral index measurements, a galaxy's effective radius,  $R_e$ , and the ellipticity within it,  $\epsilon_e$ .

### 2.3 Data sample

There are currently 2,777 galaxies observed by the MaNGA survey and consequently observed by SDSS. We cross-matched these galaxies with a radius of  $3''$  to the GALEX survey in order to obtain NUV photometry (see Section 2.1), resulting in 1,413 galaxies.

In this study we wish to study the quenching histories of these galaxies, therefore we sub-select those galaxies which are below the SFS. Here we utilise the global average SFR values quoted in the MPA-JHU catalogue (Kauffmann et al. 2003; Brinchmann et al. 2004, which are corrected for aperture bias). We do not utilise the MaNGA spectra to calculate SFRs since the bundles only extend to  $1.5 R_e$ , which would result in an underestimation of the global SFR of a galaxy.

We select galaxies with a SFR more than  $1\sigma$  below the SFS of Peng et al. (2010). Since we wish to test whether non-regular rotators quench at rapid rates consistent with major mergers, we wish to include those galaxies which have just left the SFS (rather than selection those that are, for example,  $3\sigma$  below the SFS). This selection on SFR when applied to the MANGA-GALEX sample results in a sample of 838 quenching or quenched galaxies, which we will refer to as the Q-MANGA-GALEX sample.

Note that this selection will induce some bias in our sample. Regular rotators are theorised to evolve through processes which provide a fresh supply of gas for star formation, including gas-rich mergers and gas accretion, whereas non-regular rotators are thought to only form through dry major mergers. If this is the case, then a non-regular rotator can only be formed from a regular rotator within which quenching is already under way. We must therefore be aware of this caveat when analysing the results found in this investigation.

In order to classify the galaxies in the Q-MANGA-GALEX sample as regular rotators or otherwise, we use the equation for specific stellar angular momentum as defined by Emsellem et al. (2007, 2011);

$$\lambda_{R_e} = \frac{\sum_{i=1}^N F_i R_i |V_i|}{\sum_{i=1}^N F_i R_i (V_i^2 + \sigma_i^2)^{1/2}}, \quad (1)$$

where  $F_i$  is the flux in the  $i$ th spaxel,  $R_i$  the spaxel's distance from the galaxy centre (where  $R_i < R_e$ , the effective radius of a galaxy),  $V_i$  the mean stellar velocity in that spaxel,  $\sigma_i$  the stellar velocity dispersion in that spaxel and  $N$  the total number of spaxels. In this work we use the python function provided in the MaNGA DAP to calculate  $\lambda_{R_e}$  using the values of mean flux, radius, stellar velocity and stellar velocity dispersion (corrected for instrumental resolution effects) provided by the MaNGA DAP (see Section 2.2). Velocity dispersion measurements in each spaxel of a galaxy were confirmed to be above the instrument resolution of  $77 \text{ km s}^{-1}$ .

We classify galaxies in the Q-MANGA-GALEX sample as regular or non-regular rotators using the definition from Cappellari (2016):

$$\lambda_{R_e} < 0.08 + \frac{\epsilon_e}{4} \quad \text{with} \quad \epsilon_e < 0.4. \quad (2)$$

Using this definition reveals 673 (80%) regular rotators and 157 (20%) non-regular rotators in the Q-MANGA-GALEX sample.

In order to control for the degeneracies between mass,

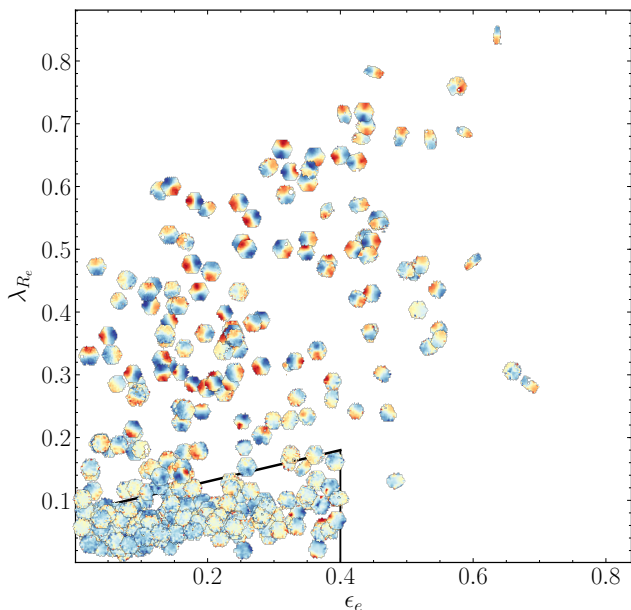


**Figure 1.** Ellipticity versus stellar angular momentum for the mass matched regular and non-regular rotators of the MM-Q-MANGA-GALEX sample. Each point is shown by its stellar velocity map, each normalised to have the midpoint, between maximum and minimum measured velocity dispersions, shown by the colour yellow. We show the separation between regular (i.e. fast) and non-regular (i.e. slow) rotators from Cappellari (2016) with the solid black line.

metallicity and dust we selected a sub-sample of regular rotators matched to within  $\pm 2.5$  pc of the stellar mass of the non-regular rotators to give 157 regular rotators. We shall refer to this sample of 314 galaxies as the MM-Q-MANGA-GALEX sample. An Anderson-Darling (AD) test reveals that the distribution of stellar masses of the non-regular rotators and regular rotators within this sample are statistically indistinguishable ( $p = 0.28$ ). Similarly their redshift distributions are also statistically indistinguishable ( $p = 0.34$ ). Therefore the only difference between the regular and non-regular rotators of the MM-Q-MANGA-GALEX sample is their kinematics. This is highlighted by their velocity maps shown in Figure 1 along with the definition of a non-regular rotator from Cappellari (2016), shown by the solid black line.

## 2.4 SFH Inference

STARPY<sup>1</sup> is a PYTHON code which allows the inference of the exponentially declining star formation history (SFH) of a single galaxy using Bayesian Markov Chain Monte Carlo techniques (Foreman-Mackey et al. 2013)<sup>2</sup>. The code uses the solar metallicity stellar population models of (Bruzual & Charlot 2003, hereafter BC03), assumes a Chabrier IMF (Chabrier 2003) and requires the input of the observed  $u-r$  and  $NUV-u$  colours and redshift. No attempt is made to model for intrinsic dust.

The SFH is described by an exponentially declining

SFH described by two parameters; the time at the onset of quenching,  $t_q$  [Gyr], and the exponential rate at which quenching occurs,  $\tau$  [Gyr]. Under the simplifying assumption that all galaxies formed at  $t = 0$  Gyr with an initial burst of star formation, the SFH can be described as:

$$SFR = \begin{cases} i_{sfr}(t_q) & \text{if } t < t_q \\ i_{sfr}(t_q) \times \exp\left(\frac{-(t-t_q)}{\tau}\right) & \text{if } t > t_q \end{cases} \quad (3)$$

where  $i_{sfr}$  is an initial constant star formation rate dependent on  $t_q$  (Schawinski et al. 2014; Smethurst et al. 2015). A smaller  $\tau$  value corresponds to a rapid quench, whereas a larger  $\tau$  value corresponds to a slower quench. Note that a galaxy undergoing a slow quench is not necessarily quiescent by the time of observation. Similarly, despite a rapid quenching rate, star formation in a galaxy may still be ongoing at very low rates, rather than being fully quenched. This SFH model has previously been shown to appropriately characterise quenching galaxies (Weiner et al. 2006; Martin et al. 2007; Noeske et al. 2007; Schawinski et al. 2014).

We assume a flat prior on all the model parameters and model the difference between the observed and predicted  $u-r$  and  $NUV-u$  colours as independent realisations of a double Gaussian likelihood function (Equation 2 in Smethurst et al. 2015). We also make the simplifying assumption that the age of each galaxy,  $t_{age}$  corresponds to the age of the Universe at its observed redshift,  $t_{obs}$ .

The probabilistic fitting methods to these star formation histories for an observed galaxy are described in full detail in Section 3.2 of Smethurst et al. (2015), wherein the STARPY code was used to characterise the morphologically dependence of the SFHs of  $\sim 126,000$  galaxies. Similarly, in Smethurst et al. (2016), STARPY was used to show the prevalence of rapid, recent quenching within a population of AGN host galaxies and in Smethurst et al. (2017) to investigate the quenching histories of group galaxies.

An example posterior probability distribution output by STARPY is shown for a single galaxy in Figure 5 of Smethurst et al. (2015), wherein the degeneracies of the SFH model between recent, rapid quenching and earlier, slower quenching can clearly be seen.

To study the SFH across a sample of many galaxies, these individual posterior probability distributions are stacked in  $[t_q, \tau]$  space to give a single distribution for the sample. This is no longer inference but merely a method to visualise the results for a population of galaxies (see appendix section C in Smethurst et al. 2016 for a discussion on alternative methods which may be used to determine the parent population SFH). These distributions will be referred to as the population SFH densities.

## 3 RESULTS

We determine the population SFH densities for both the regular and non-regular rotators of the MM-Q-MANGA-GALEX sample. This is shown in Figure 2 for both the time that quenching occurs (left panel) and exponential rate of quenching (right panel) for the regular (black solid line) and non-regular (red dashed line) rotators. Uncertainties on the population densities (shown by the shaded regions) are determined from the maximum and minimum values spanned by  $N = 1000$  bootstrap iterations, each sampling 90% of

<sup>1</sup> Publicly available: <http://github.com/zoouniverse/starpy>

<sup>2</sup> <http://dan.iel.fm/emcee/>

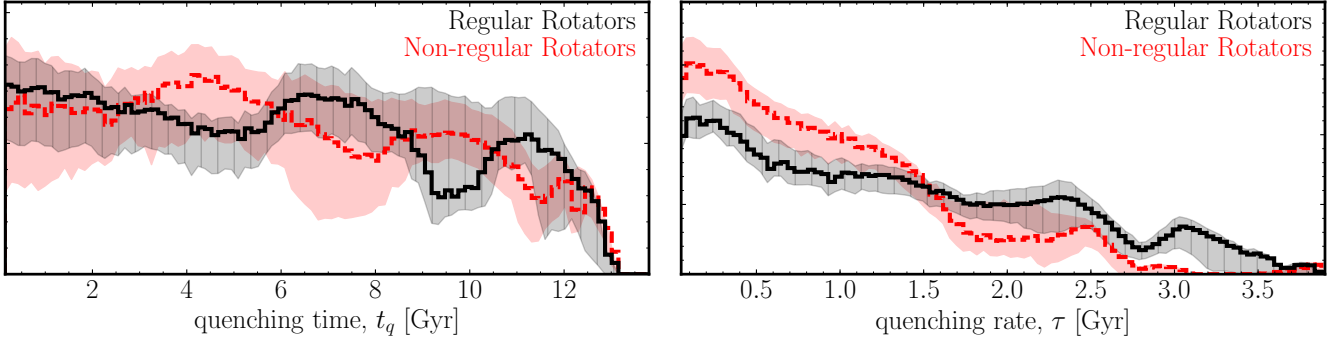


**Figure 2.** Population densities for the time,  $t_q$  (left) and exponential rate,  $\tau$  (right) that quenching occurs in the MM-Q-MANGA-GALEX sample for the regular (black, solid) and non-regular (red, dashed) rotators. A high value of  $t_q$  corresponds to a recent quench, and a high value of  $\tau$  corresponds to a slow quench. Shaded regions show the uncertainties on the distributions from bootstrapping. An AD-test between the  $t_q$  distributions revealed that we cannot reject ( $p = 0.49$ ) the null hypothesis that the regular and non-regular rotators quench at the same time. However, an AD-test between the  $\tau$  distributions revealed that we can reject ( $p = 0.0003$ ) the hypothesis that the regular and non-regular rotators quench at the same rate. This is a  $3.6\sigma$  result, suggesting that non-regular rotators quench more rapidly than regular rotators of the same mass.

either the regular (black shaded region) or non-regular (red shaded region) rotators.

To statistically test the significance of our results, we estimate the ‘best fit’  $[t_q, \tau]$  values for each galaxy with the median value of an individual galaxy’s posterior probability distribution from STARPY (i.e. the 50th percentile position of the MCMC chain). We test the distribution of these values of the regular and non-regular rotators in the MM-Q-MANGA-GALEX sample with Anderson-Darling (AD) tests. Firstly, an AD-test on the distribution of  $t_q$  values for each galaxy, revealed that we cannot reject the null hypothesis that the regular and non-regular rotators quench at the same time ( $p \sim 0.49$ ). Finally, an AD-test on the distribution of  $\tau$  values for each galaxy, revealed that we can reject the null hypothesis that the fast and slow rotators quench at the same rate ( $p \sim 0.0003$ ). This is a statistically significant ( $3.6\sigma$ ) result, suggesting that non-regular rotators quench more rapidly than regular rotators of the same mass.

## 4 DISCUSSION

The results shown in Figure 2 suggest that regular and non-regular rotators are indeed separate populations quenched, and therefore formed, by different mechanisms. However, these quenching mechanisms appear to occur at similar cosmic times for regular and non-regular rotators.

Our results contradict the results of the simulations of Khochfar et al. (2011) who find that the last major merger interaction for slow rotators was at  $z \gtrsim 1.5$  (i.e.  $t_q \lesssim 4.5$  Gyr). Contradicting the findings of Khochfar et al., Penoyre et al. (2017) find in the Illustris simulation that slow rotators only form after  $z < 1$  (i.e.  $t_q \gtrsim 6$  Gyr). We note that STARPY is not very sensitive to the time of quenching, particularly at early times i.e.  $t_q \lesssim 6$  Gyr when  $z \gtrsim 1$ . Therefore, with STARPY in its current form we cannot currently conclude which scenario our results favour. Future work altering our inference code to take spatial spectral information provided by MaNGA may help us to address this issue.

We find that a fraction of the regular rotator sample quench at very slow rates ( $\tau \gtrsim 3$  Gyr; right panel of Fig-

ure 2). Since the Q-MANGA-GALEX sample has not been selected by visual morphology, there will be regular rotators which are disc dominated (i.e. with bulge-to-total mass ratios of less than 0.5 which would historically have been classified as a late-type galaxy). This likelihood for slower quenching rates is therefore likely to be caused by the effects of secular evolution through gas accretion, slowly quenching these disk galaxies off the SFS. Using the morphological classifications of Galaxy Zoo 2 (Lintott et al. 2011; Willett et al. 2013) we find that  $\sim 31\%$  of the regular rotators of the Q-MANGA-GALEX sample have a disk or featured debiased vote fraction,  $p_d \geq 0.8$  (i.e. 80% of classifiers marked the galaxy as having either a disk or features), and a debiased merger vote fraction,  $p_{\text{merger}} < 0.223$  (i.e. is not currently undergoing a merger). This is consistent with the fact that  $26.0 \pm 3.4\%$  of the regular rotator quenching rate population density (black line in the right panel of Figure 2) is found at quenching rates  $\tau > 2$  Gyr. Conversely only 9 non-regular rotators ( $\sim 5\%$ ) were classified as having a disk or features, and of these galaxies 6 have a debiased odd vote fraction,  $p_{\text{odd}} \geq 0.3$ , suggesting they are undergoing either an interaction or merger. Upon visual inspection, the other 3 are large disks with spiral structures lying outside of the MaNGA fibre bundle at  $> 1.5 R_e$ .

The prevalence of rapid rates in the non-regular rotators of the Q-MANGA-GALEX sample supports the theory that these galaxies are formed by major mergers, which are thought to cause quenching at such rates (Springel et al. 2005; Bell et al. 2006; Lotz et al. 2008, 2011; Smethurst et al. 2015). However, we also find evidence for regular rotators quenching at these same rapid rates. Simulations have recently shown that although major mergers can cause rapid quenching of a galaxy, they do not necessarily destroy the disk dominated nature of a galaxy (Pontzen et al. 2016; Sparre & Springel 2016). This is thought to mainly occur in gas rich major mergers and is likely the explanation for the preference for rapid rates in the regular rotator sample seen in Figure 2.

Our results suggest that although the kinematics of regular and non-regular rotators are different in nature, the mechanisms which quench, and therefore evolve, these



galaxies are very similar. However, in order to completely destroy the disk of a galaxy, some property in the formation/quenching mechanism must exceed some threshold. Since simulations have shown that it is possible for a disc to be retained in a major 1:1 mass ratio merger, this quantity cannot be the merger mass ratio as previously thought (Binney & Tremaine 1987; Bois et al. 2010; Tonini et al. 2016). Instead, our results showing similar quenching rates occurring across both regular and non-regular rotator samples, combined with the findings of recent simulations by Pontzen et al. (2016); Sparre & Springel (2016), suggest that the total gas mass fraction within a pair of merging galaxies, is what will ultimately decide the kinematic fate of a galaxy.

## REFERENCES

- Abazajian K. N. et al., 2009, *ApJS*, 182, 543  
 Bell E. F., Phleps S., Somerville R. S., Wolf C., Borch A., Meisenheimer K., 2006, *ApJ*, 652, 270  
 Binney J., Tremaine S., 1987, *Galactic dynamics*  
 Blanton M. R., Eisenstein D., Hogg D. W., Schlegel D. J., Brinkmann J., 2005, *ApJ*, 629, 143  
 Blanton M. R., Roweis S., 2007, *AJ*, 133, 734  
 Bois M. et al., 2010, *MNRAS*, 406, 2405  
 Brinchmann J., Charlot S., White S. D. M., Tremonti C., Kauffmann G., Heckman T., Brinkmann J., 2004, *MNRAS*, 351, 1151  
 Bruzual G., Charlot S., 2003, *MNRAS*, 344, 1000  
 Bundy K. et al., 2015, *ApJ*, 798, 7  
 Cappellari M., 2016, *ARA&A*, 54, 597  
 Cappellari M. et al., 2007, *MNRAS*, 379, 418  
 Cappellari M. et al., 2013, *MNRAS*, 432, 1862  
 Cardelli J. A., Clayton G. C., Mathis J. S., 1989, *ApJ*, 345, 245  
 Chabrier G., 2003, *PASP*, 115, 763  
 Cheung E. et al., 2012, *ApJ*, 760, 131  
 Drory N. et al., 2015, *AJ*, 149, 77  
 Duc P.-A. et al., 2011, *MNRAS*, 417, 863  
 Emsellem E. et al., 2011, *MNRAS*, 414, 888  
 Emsellem E. et al., 2007, *MNRAS*, 379, 401  
 Fang J. J., Faber S. M., Koo D. C., Dekel A., 2013, *ApJ*, 776, 63  
 Foreman-Mackey D., Hogg D. W., Lang D., Goodman J., 2013, *PASP*, 125, 306  
 Gunn J. E. et al., 2006, *AJ*, 131, 2332  
 Hayward C. C., Torrey P., Springel V., Hernquist L., Vogelsberger M., 2014, *MNRAS*, 442, 1992  
 Hopkins P. F., Cox T. J., Kereš D., Hernquist L., 2008a, *ApJS*, 175, 390  
 Hopkins P. F., Hernquist L., Cox T. J., Di Matteo T., Robertson B., Springel V., 2006, *ApJS*, 163, 1  
 Hopkins P. F., Hernquist L., Cox T. J., Kereš D., 2008b, *ApJS*, 175, 356  
 Jarosik N. et al., 2011, *ApJS*, 192, 14  
 Johnston E. J., Aragón-Salamanca A., Merrifield M. R., 2014, *MNRAS*, 441, 333  
 Kauffmann G. et al., 2003, *MNRAS*, 341, 33  
 Khochfar S. et al., 2011, *MNRAS*, 417, 845  
 Khochfar S., Silk J., 2009, *MNRAS*, 397, 506  
 Law D. R. et al., 2016, *AJ*, 152, 83  
 Law D. R. et al., 2015, *AJ*, 150, 19  
 Lintott C. et al., 2011, *MNRAS*, 410, 166  
 Lotz J. M., Jonsson P., Cox T. J., Croton D., Primack J. R., Somerville R. S., Stewart K., 2011, *ApJ*, 742, 103  
 Lotz J. M., Jonsson P., Cox T. J., Primack J. R., 2008, *MNRAS*, 391, 1137  
 Martin D. C. et al., 2005, *ApJ*, 619, L1  
 Martin D. C. et al., 2007, *ApJS*, 173, 342  
 Mihos J. C., Hernquist L., 1994, *ApJ*, 431, L9  
 Naab T. et al., 2014, *MNRAS*, 444, 3357  
 Noeske K. G. et al., 2007, *ApJ*, 660, L43  
 Oh K., Sarzi M., Schawinski K., Yi S. K., 2011, *ApJS*, 195, 13  
 Padmanabhan N. et al., 2008, *ApJ*, 674, 1217  
 Peng Y.-j. et al., 2010, *ApJ*, 721, 193  
 Penoyre Z., Moster B. P., Sijacki D., Genel S., 2017, *ArXiv e-prints*, 1703.00545  
 Pontzen A., Tremmel M., Roth N., Peiris H. V., Saintonge A., Volonteri M., Quinn T., Governato F., 2016, *ArXiv e-prints*, 1607.02507  
 Schawinski K. et al., 2014, *MNRAS*, 440, 889  
 Smee S. A. et al., 2013, *AJ*, 146, 32  
 Smethurst R. J., Lintott C. J., Bamford S. P., Hart R. E., Kruk S. J., Masters K. L., Nichol R. C., Simmons B. D., 2017, *ArXiv e-prints*, 1704.06269  
 Smethurst R. J. et al., 2016, *MNRAS*, 463, 2986  
 Smethurst R. J. et al., 2015, *MNRAS*, 450, 435  
 Snyder G. F., Cox T. J., Hayward C. C., Hernquist L., Jonsson P., 2011, *ApJ*, 741, 77  
 Sparre M., Springel V., 2016, *ArXiv e-prints*, 1610.03850  
 Springel V., Di Matteo T., Hernquist L., 2005, *ApJ*, 620, L79  
 Stott J. P. et al., 2016, *MNRAS*, 457, 1888  
 Stoughton C. et al., 2002, *AJ*, 123, 485  
 Tonini C., Mutch S. J., Croton D. J., Wyithe J. S. B., 2016, *MNRAS*, 459, 4109  
 Toomre A., Toomre J., 1972, *ApJ*, 178, 623  
 Weiner B. J. et al., 2006, *ApJ*, 653, 1049  
 Willett K. W. et al., 2013, *MNRAS*, 435, 2835  
 Yan R. et al., 2016, *AJ*, 152, 197  
 York D. G. et al., 2000, *AJ*, 120, 1579